

Analysis of confined seepage flow using the scaled boundary finite-element method



Mohammad Hossein Bazayar*, Adel Graïli*, Chongmin Song**

*Department of Civil Engineering, Yasouj University, Yasouj, Iran

**School of Civil and Environmental Engineering, University of New South Wales, Sydney, NSW 2052, Australia

ABSTRACT

The scaled boundary finite-element method (SBFEM) a recently developed semi-analytical technique is applied to the analysis of confined seepage flow. This method combines the advantages of the finite-element method and boundary element method. In this scheme only the boundary of the domain is discretized, no fundamental solution is required and singularity problems can be modeled rigorously. Anisotropic and non-homogeneous materials satisfying similarity are modeled without additional efforts. In this paper, SBFE equations and the solution procedures for the analysis of confined seepage flow are outlined. The accuracy, effectiveness and efficiency of the proposed method are demonstrated by modelling seepage flow under a sheet pile wall and a concrete dam with a cut-off at heel.

RÉSUMÉ

La limite échelon méthode des éléments finis (SBFEM), qui est une nouvelle technique semi-analytique et combinant les avantages de la méthode des éléments finis et la méthode des éléments de frontière, est appliquée à l'analyse du flux d'infiltration confiné. Dans cette méthode, aucune solution de fond n'est nécessaire et les problèmes de singularité peuvent être modélisés de façon rigoureuse. Anisotrope et des matériaux non-homogènes satisfaisant similitude sont modélisés sans efforts supplémentaires. Dans cet article, des équations et des procédures SBFE solution pour l'analyse des flux d'infiltration limitée sont décrites. La précision et l'efficacité de la méthode proposée sont démontrées par l'infiltration de modélisation sous un rideau de palplanches et un barrage en béton avec une teneur de coupure au niveau du talon.

1 INTRODUCTION

Calculating the quantity of water flowing through a soil and the forces associated with this flow is crucial to the design of various civil engineering structures such as foundations, earth dams, concrete dams, and retaining walls. This field of study has attracted the attention of many geotechnical engineering researchers. To analyze seepage flow, analytical solutions, graphical solutions, electrical analogies and numerical simulations have been employed. Analytical solutions are limited to the problems of simple geometry and material property. However, because of limitations associated with closed form solutions, in many cases seepage flow analysis is simulated numerically. The most widely used numerical techniques are the finite-element method (FEM), the boundary element method (BEM) and the finite-difference method (FDM). A brief existing literature on the applications of the above mentioned numerical techniques in seepage flow analysis is presented in the following.

Brebbia and Chang (1979) used the boundary element method to analyze seepage flow in porous media such as foundation of concrete dams. The results of their study showed the range of applications of the technique. In general, the results obtained using the boundary elements method tend to be more accurate than those modeled by finite elements. This study demonstrated that the computational cost of the

boundary element method is much less than the finite-element method.

Fan and Tompkins (1992) presented a simple and unique method for generating flow nets based on nodal potentials and bilinear shape functions. The method reduces the work of performing a second FEM to compute the stream potentials at the nodes.

Chen et al. (1993) derived a dual integral formulation with a hyper-singular integral to solve the boundary value problem with singularity arising from a degenerate boundary. They analyzed a seepage flow under a dam with sheet piles to check the validity of the mathematical model. Finally, four design cases of sheet piles were examined and the best choice was suggested. Jie et al. (2004) presented a finite-difference method based on boundary-fitted coordinate (BFC) to deal with the practical steady seepage in foundation pit, in lock foundation, and to analyze the seepage in an embankment dam with a free surface. The applications of BFC transformation method demonstrated its advantage in closely simulating the problems with complex boundaries.

Each of these numerical methods has their own merits and drawbacks and generally speaking, which of them is better depends on the specified problem involved. Some of the defects associated with these numerical techniques are outlined in the following.

The FEM has to truncate the computational domain when dealing with unbounded domain problems leading to a reduction in accuracy. For modelling the stress

singularity in the vicinity of sharp re-entrant corners the FEM solution converges rather slowly. Moreover in FEM the whole computational domain has to be discretized. The FDM usually requires a structured grid. Consequently, coordinate-mapping techniques or adaptive meshing algorithms are needed to solve problems with complicated geometries. In addition, there is no straight-forward way to test the accuracy of a solution and the scheme is prone to certain types of numerical instabilities. The FDM is also unable to handle sharp re-entrant corners very well, and like the FEM the whole domain must be discretized. The BEM needs to evaluate singular integrals which can be very complicated at times. Also in this method the matrix of the linear algebraic equation system is dense resulting in an increase in computational costs. Moreover, the BEM suffers numerical difficulties when modeling near sharp re-entrant corners and finding fundamental solutions for non-homogeneous and anisotropic media is so complicated and sometimes even impossible.

It is the goal of this paper to apply the so-called scaled boundary finite-element method to the analysis of seepage flow around re-entrant corners. As will become apparent the restrictions of the other procedures mentioned in the previous paragraph are not present in this method.

2 SCALED BOUNDARY FINITE-ELEMENT METHOD

The scaled boundary finite-element method, a fundamental-solution-less boundary element method, is an attractive alternative to the numerical schemes in computational mechanics. It not only combines some important advantages of the finite-element and boundary element methods but also has its own salient features. The method was developed by Wolf and Song (1996). In recent years, further development of the method has been performed for different fields of physics, such as elastomechanics (Lindemann and Becker 2002), diffusion (Song and Wolf 1999), potential flow (Deeks and Cheng 2003) and wave propagation (Bazyar and Song 2008). The SBFEM is based on the finite-element technology so that it does not require fundamental solutions. The radiation condition at infinity is satisfied rigorously. Like the boundary element method only the boundary is discretized reducing the spatial discretization by one and leading to the increase of computational efficiency. Problems involving stress singularities and discontinuities can be modeled accurately. Anisotropic media can be handled without additional computational efforts. In the scaled boundary finite-element method, a so-called scaling center O is chosen in a zone from which the total boundary other than the straight surfaces passing through the scaling center must be visible (See Figure 1.a). Only the boundary S directly visible from the scaling center O is discretized as shown in Figure 1.a. In two dimensional problems one-dimensional line elements are used (Figure 1.b). The straight surfaces passing through the scaling center (side faces) and the interfaces between different materials are not discretized (Figure

1.a). The geometry of an element on the boundary is interpolated using the shape functions in the same way as in the finite-element method. The geometry of the domain V is described by scaling the boundary with the dimensionless radial coordinate ξ pointing from the scaling center to a point on the boundary (Figure 1.a). The radial and circumferential coordinates ξ and η form the *scaled boundary coordinates*. As the local coordinate η form the boundary, the shape functions only depend on the circumferential coordinate η which is defined within a range $-1 \leq \eta \leq 1$. The dimensionless radial coordinate ξ is defined within a range $0 \leq \xi \leq 1$ for bounded domains and $1 \leq \xi < \infty$ for unbounded domains.

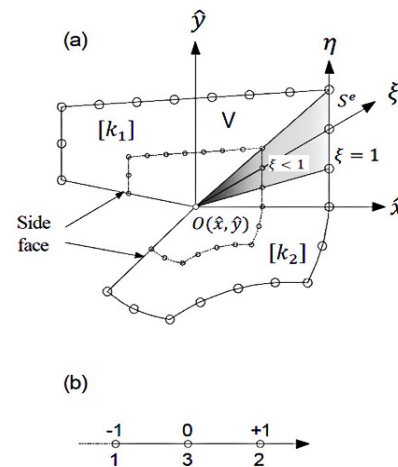


Figure 1. (a) Spatial discretization for a bounded domain in the scaled boundary finite-element method; (b) three-node line elements to be used on the boundary

In this method the governing equations are handled in the strong form in the radial direction and in the weak form in the other directions, which form the boundary of the considered domain. The weak form is treated by a finite-element approximation and the strong form leads to a set of ordinary differential equations being solved via an eigen-value problem. The solution procedure leads to a boundary stiffness matrix giving the linear relation between nodal heads and fluxes on the boundary. In a second step, the potential heads within the domain can be calculated analytically with the knowledge of the heads on the boundary.

3 SEEPAGE ANALYSIS USING THE SCALED BOUNDARY FINITE-ELEMENT METHOD

In this section firstly, governing equations for seepage problems are summarized. Secondly, scaled boundary finite-element formulation for two dimensional seepage problems is presented.

3.1 Governing equations for seepage problems

Seepage flow in two-dimensional problems is governed by the Laplace equation. If we present the potential

function by $\phi(x, y) = kh(x, y)$, the Laplace equation may be expressed as

$$\nabla^2 \phi(x, y) = 0 \quad [1]$$

Using the relation between the potential head and the velocity in two directions, the velocity vector is expressed as

$$v = -\nabla \phi(x, y) \quad [2]$$

On the boundary of the domain either the value of the potential or the flow velocity must be specified. Designating the entire boundary by Γ , the potential boundary by Γ_ϕ and the velocity boundary by Γ_v , the boundary conditions may be specified as

$$\phi = \bar{\phi} \quad \text{on } \Gamma_\phi \quad [3]$$

$$\frac{\partial \phi}{\partial n} = -\bar{v} \quad \text{on } \Gamma_v \quad [4]$$

3.2 Scaled boundary finite-element formulation

As mentioned in Section 2, in the scaled boundary finite-element method, the geometry of the domain must be transformed from Cartesian coordinates to the scaled boundary coordinates. A typical boundary element on the part of the boundary S^e (superscript e for element) is shown in Figure 1.a. For a two-dimensional problem, the nodal coordinates of an element in the Cartesian coordinate system are arranged in $\{x\}$, $\{y\}$. The geometry of the isoparametric boundary element is interpolated using the shape functions $[N(\eta)]$ formulated in the local coordinate η , as

$$x(\eta) = [N(\eta)]\{x\} \quad [5.a]$$

$$y(\eta) = [N(\eta)]\{y\} \quad [5.b]$$

A point (\hat{x}, \hat{y}) inside the domain V is expressed as

$$\hat{x} = \hat{x}_0 + \xi x(\eta) = \hat{x}_0 + \xi [N(\eta)]\{x\} \quad [6.a]$$

$$\hat{y} = \hat{y}_0 + \xi y(\eta) = \hat{y}_0 + \xi [N(\eta)]\{y\} \quad [6.b]$$

Using the above transformations, the geometry of the domain is transformed to the scaled boundary coordinates. Along the radial lines passing through the scaling center O and a node on the boundary, the nodal

head functions $\{\phi_h(\xi)\}$ are introduced. The potential head at a node (ξ, η) is interpolated from potential head functions $\{\phi_h(\xi)\}$ as shown in Figure 2.

$$\{\phi_h(\xi, \eta)\} = [N(\eta)]\{\phi_h(\xi)\} \quad [7]$$

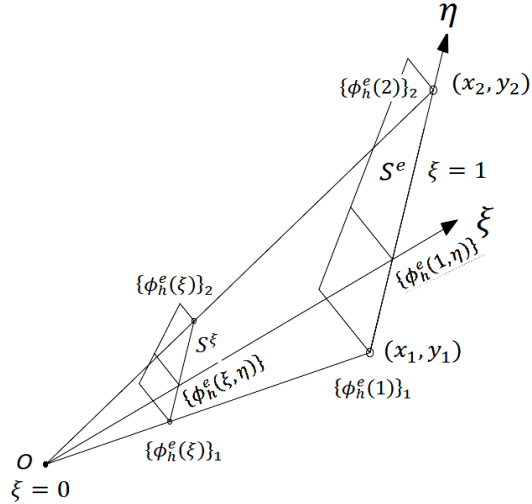


Figure 2. Potential heads in domain by interpolation of nodal potential head functions

Using conventional techniques, the operator ∇ can be mapped to the scaled boundary coordinates (Deeks and Cheng 2003) as

$$\nabla = [b^1(\eta)] \frac{\partial}{\partial \xi} + [b^2(\eta)] \frac{1}{\xi} \frac{\partial}{\partial \eta} \quad [8]$$

where $[b^1(\eta)]$ and $[b^2(\eta)]$ are dependent only on the boundary of the domain. Substituting Eqs. 7 and 8 into Eq. 2, the approximate velocities can be expressed in terms of the scaled boundary coordinates as

$$\{v_h(\xi, \eta)\} = -[B^1(\eta)]\{\phi_h(\xi)\}_{,\xi} - \frac{1}{\xi} [B^2(\eta)]\{\phi_h(\xi)\} \quad [9]$$

where

$$[B^1(\eta)] = [b^1(\eta)] [N(\eta)] \quad [10.a]$$

$$[B^2(\eta)] = [b^2(\eta)] [N(\eta)]_{,\eta} \quad [10.b]$$

The weighted residual method is employed to perform the finite-element approximation and derive the scaled boundary finite-element equations for seepage flow. Applying the weighted residual method to the governing

equations and introducing the following coefficient matrices

$$[E^0] = \int_{\eta} [B^1(\eta)]^T [k][B^1(\eta)] J |d\eta \quad [11.a]$$

$$[E^1] = \int_{\eta} [B^2(\eta)]^T [k][B^1(\eta)] J |d\eta \quad [11.b]$$

$$[E^2] = \int_{\eta} [B^2(\eta)]^T [k][B^2(\eta)] J |d\eta \quad [11.c]$$

$$\{F_s(\xi)\} = [N(\eta_0)]^T (-\bar{v}(\xi, \eta_0)) J(\eta_0) + [N(\eta_1)]^T (-\bar{v}(\xi, \eta_1)) J(\eta_1) \quad [11.d]$$

the scaled boundary finite-element equation for seepage flow is derived as

$$[E^0] \xi^2 \{\phi_h(\xi)\}_{,\xi\xi} + ([E^0] + [E^1]^T - [E^1]) \xi \{\phi_h(\xi)\}_{,\xi} - [E^2] \{\phi_h(\xi)\} = \xi \{F_s(\xi)\} \quad [12]$$

Hydraulic conductivity matrix [k] may be expressed as

$$[k] = \begin{bmatrix} k_x & 0 \\ 0 & k_y \end{bmatrix} \quad [13]$$

Note that the coefficient matrices $[E^0]$, $[E^1]$ and $[E^2]$ are independent of ξ . $[E^1]$ is positive definite and $[E^2]$ is symmetric. Having calculated the above coefficient matrices for one element, in the same way as in the finite-element method, the assembled coefficient matrices of the whole boundary are determined.

3.3 Solution procedures

If curve S in Figure 1.a is closed, the side faces coincide and the flow across the side faces is equal so the term $\{F_s(\xi)\}$ vanishes. This term also vanishes if the side faces are impermeable. When $\{F_s(\xi)\}$ is equal to zero, Eq. 12 becomes a homogeneous set of Euler–Cauchy differential equations as

$$[E^0] \xi^2 \{\phi_h(\xi)\}_{,\xi\xi} + ([E^0] + [E^1]^T - [E^1]) \xi \{\phi_h(\xi)\}_{,\xi} - [E^2] \{\phi_h(\xi)\} = 0 \quad [14]$$

whose solution may be found in the form

$$\{\phi_h(\xi)\} = c_1 \xi^{-\lambda_1} \{\phi_1\} + c_2 \xi^{-\lambda_2} \{\phi_2\} + \dots \quad [15]$$

where the exponents $-\lambda_i$ and corresponding vectors $\{\phi_i\}$ may be interpreted as independent modes of potential closely satisfying internal equilibrium in the ξ direction. The flows into the domain required at the boundary nodes by each potential, are expressed as

$$\{q(\xi)\} = [E^0] \xi \{\phi_h(\xi)\}_{,\xi} + [E^1]^T \{\phi_h(\xi)\} \quad [16]$$

The homogeneous second-order differential equations in Eq. 14 with n unknown potential head functions are transformed to the first-order ordinary differential equations with $2n$ unknowns by introducing the variable

$$\{X(\xi)\} = \begin{Bmatrix} \{\phi_h(\xi)\} \\ \{q(\xi)\} \end{Bmatrix} \quad [17]$$

This results in the first-order differential equations

$$\xi \{X(\xi)\}_{,\xi} = -[Z] \{X(\xi)\} \quad [18]$$

with the coefficient matrix

$$[Z] = \begin{bmatrix} [E^0]^{-1} [E^1]^T & -[E^0]^{-1} \\ -[E^2] + [E^1] [E^0]^{-1} [E^1]^T & -[E^1] [E^0]^{-1} \end{bmatrix} \quad [19]$$

$[Z]$ is a Hamiltonian matrix which occurs in the solution of algebraic Riccati equations. Substituting the formal solution of $\{X(\xi)\}$

$$\{X(\xi)\} = \xi^{-\lambda_i} \{\phi_i\} \quad [20]$$

into Eq. 18 leads to the eigen-problem of matrix $[Z]$ as

$$[Z] \{\phi_i\} = \lambda_i \{\phi_i\} \quad [21]$$

The eigen-values and eigen-vector matrices are partitioned conformably as

$$[Z][\Phi] = [\Phi][\lambda] = \begin{bmatrix} [\Phi_{h1}] & [\Phi_{h2}] \\ [\Phi_{q1}] & [\Phi_{q2}] \end{bmatrix} \begin{bmatrix} [\lambda_n] \\ [\lambda_p] \end{bmatrix} \quad [22]$$

The real parts of all terms of $[\lambda_n]$ are negative and of $[\lambda_p]$ are positive. With the transformed functions $\{w(\xi)\}$ defined in $\{X(\xi)\} = [\Phi]\{w(\xi)\}$, the transformation in Eq. 22 decouples Eq. 18 as

$$\xi w_i(\xi)_{,\xi} = -\lambda_i w_i(\xi) \quad [23]$$

whose general solution is equal to $w_i(\xi) = c_i \xi^{-\lambda_i}$. Using this solution, definition of $\{w(\xi)\}$ and the partition of the eigen-values and eigen-vectors in Eq. 22, the solution of Eq. 18 is written as

$$\{X(\xi)\} = \begin{bmatrix} [\Phi_{h1}] & [\Phi_{h2}] \\ [\Phi_{q1}] & [\Phi_{q2}] \end{bmatrix} \begin{bmatrix} \xi^{-[\lambda_n]} \\ \xi^{-[\lambda_p]} \end{bmatrix} \begin{Bmatrix} \{c_1\} \\ \{c_2\} \end{Bmatrix} \quad [24]$$

The general solutions for potential heads and nodal internal fluxes are obtained from Eqs. 17 and 24 as

$$\{\phi_h(\xi)\} = [\Phi_{h1}] \xi^{-[\lambda_n]} \{c_1\} + [\Phi_{h2}] \xi^{-[\lambda_p]} \{c_2\} \quad [25.a]$$

$$\{q(\xi)\} = [\Phi_{q1}] \xi^{-[\lambda_n]} \{c_1\} + [\Phi_{q2}] \xi^{-[\lambda_p]} \{c_2\} \quad [25.b]$$

To obtain a finite solution at the scaling center, $\{c_2\}$ must be equal to zero leading to

$$\{\phi_h(\xi)\} = [\Phi_{h1}] \xi^{-[\lambda_n]} \{c_1\} \quad [26.a]$$

$$\{q(\xi)\} = [\Phi_{q1}] \xi^{-[\lambda_n]} \{c_1\} \quad [26.b]$$

Relation between potential head and flux, on the boundary is expressed as

$$\{q(\xi = 1)\} = [K]\{\phi_h(\xi = 1)\} \quad [27]$$

The stiffness matrix on the boundary is obtained by substituting Eqs. 26.a and 26.b into Eq. 27 as

$$[K] = [\Phi_{q1}][\Phi_{h1}]^{-1} \quad [28]$$

Once the nodal potentials are determined through Eqs. 27 and 28, the entire potential field can be calculated by Eqs. 26.a and 26.b.

4 NUMERICAL EXAMPLES

Several examples were examined to verify the accuracy and applicability of the method. However in an attempt to be concise the results and discussions presented here will focus on the problems of seepage beneath a sheet pile wall through anisotropic materials and seepage under a concrete dam with a cut-off at heel constructed on a foundation consisting of non-homogeneous and anisotropic materials. A computer program in *Matlab* has been written to implement the SBFEM formulations, and *Geo-Studio* is used for FE analyses to verify the results obtained by the SBFEM.

4.1 Seepage beneath a sheet pile wall

A sheet pile wall embedded in an anisotropic soil is addressed in Figure 3. The base width is 12m, total hydraulic head difference is 9m and sheet pile embedment depth is 3m. The adopted SBFEM mesh is shown in Figure 4. Only one bounded domain is used. Scaling center is located at the bottom of the sheet pile. The embedded part of the sheet pile is not discretized. The horizontal and vertical coefficients of permeability are equal to 3×10^{-5} m/s and 1×10^{-5} m/s, respectively.

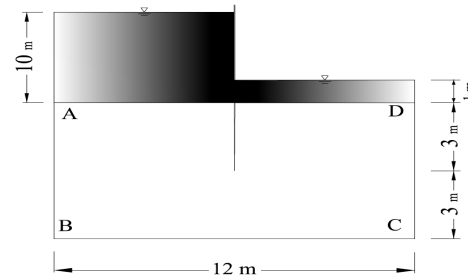


Figure 3. A sheet pile wall in an anisotropic soil

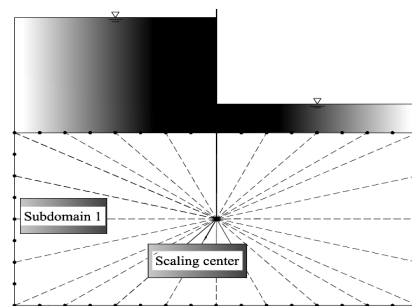


Figure 4. The scaled boundary finite element mesh for seepage flow beneath a sheet pile wall

Figure 5.a displays the seepage velocity along the line ABCD and Figure 5.b displays the seepage velocity about the perimeter of the sheet pile. As is shown in Figure 5.a there is a good agreement between the results of SBFEM and FEM along the line ABCD.

Figure 5.b shows that the SBFEM accurately models the singularity point. As shown in this figure, despite refining the mesh in FEM, the solutions lack convergence. Finally, the equipotential lines obtained using the SBFEM and FEM are compared in Figure 6. Excellent agreement can be observed.

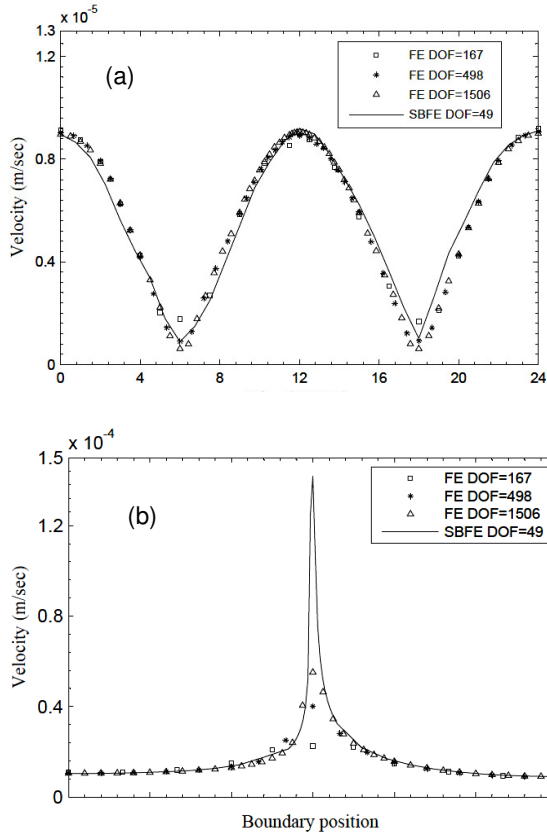


Figure 5. Seepage velocity beneath a sheet pile wall: (a) along line ABCD; (b) along perimeter of the sheet pile

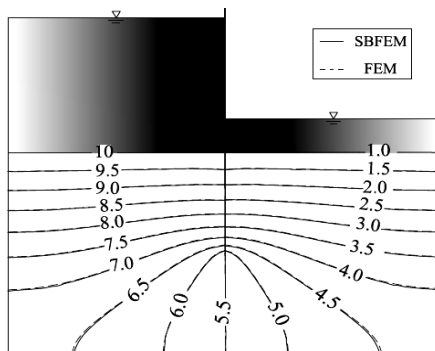


Figure 6. Equipotential lines beneath a sheet pile wall

4.2 Seepage under a concrete dam with a cut-off at heel

A concrete dam with a cut-off at heel is portrayed in Figure 7.a. Foundation of the dam consists of a non-homogeneous and anisotropic material. The base width is 16m, the total hydraulic head difference is 3.5m and embedment depth of the cut-off is 3m. The SBFEM mesh is shown in Figure 7.b. Whole domain is modeled using two sub-domains as sub-structures. Sub-domains' scaling centers and meshes are shown. Embedment depth of the cut-off is not discretized. The horizontal and vertical coefficients of permeability from ground surface to a depth of 3m are equal to 7×10^{-5} m/s and 4×10^{-6} m/s and from a depth of 3m to 6m are equal to 3×10^{-5} m/s and 2×10^{-6} m/s, respectively.

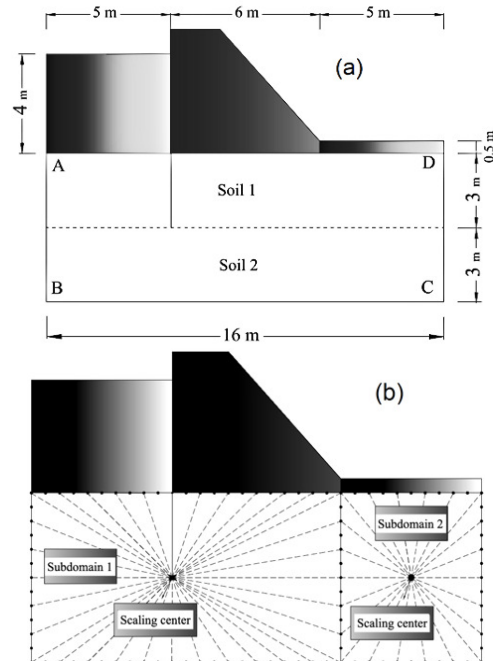
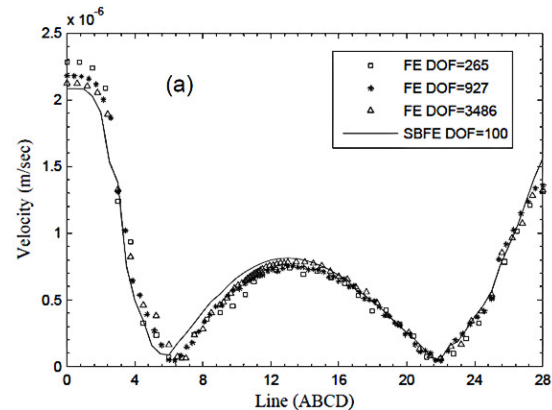


Figure 7. (a) A concrete dam with a cut-off at heel (b) scaled boundary finite element mesh



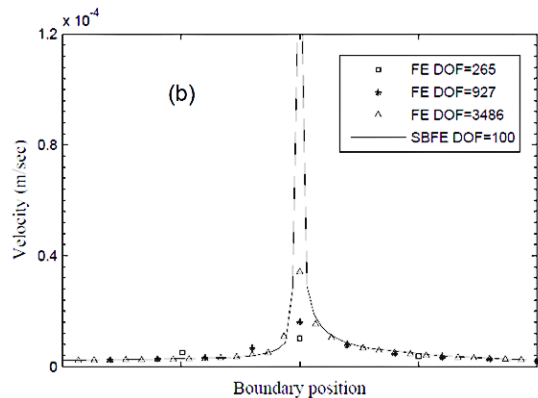


Figure 8. Seepage velocity under a concrete dam with a cut-off at heel (a) along line ABCD; (b) along perimeter of the cut-off

Seepage velocity along the line ABCD and the cut-off is presented in Figures 8.a and 8.b, respectively. Similar to the previous example, Figure 8.a shows a good agreement between the results of the two methods along the line ABCD. As is demonstrated in Figure 8.b, in contrast to the FEM, the scaled boundary finite-element method is a powerful method for modeling singularity points in the velocity domain. In Figure 9, the equipotential lines under the dam obtained using the SBFEM and the FEM are presented. This figure shows an excellent agreement between the results.

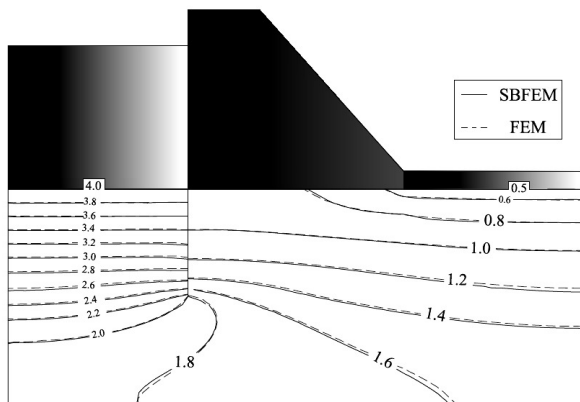


Figure 9. Equipotential lines under a concrete dam with a cut-off at heel

5 CONCLUSIONS

In this paper a new computational scheme so called the scaled boundary finite-element method is employed to analyze the confined seepage flow. This technique combines the advantages of both finite-element and boundary element methods, only the boundary is discretized, no fundamental solution is required. As only the boundary is discretized fewer elements are needed in the SBFEM than the standard FEM. Results of this study

illustrate the efficiency, accuracy and applicability of the method in modeling non-homogeneous and anisotropic domains. The results presented in this paper demonstrate that the scaled boundary finite-element method is able to accurately model the singularity of velocity field near sharp corners and out-performs the FEM.

REFERENCES

- Bazyar, M.H. and Song, Ch. 2008. A continued-fraction-based high-order transmitting boundary for wave propagation in unbounded domains of arbitrary geometry, *International Journal for Numerical Methods in Engineering*, 74: 209-237.
- Brebbia, C.A. and Chang, O.V. 1979. Boundary elements applied to seepage problems in zoned anisotropic soils, *Advances in Engineering software*, 1: 95-105.
- Chen, J.T. and Hong, H.K. and Chyuanb, S.W. 1993. Boundary element analysis and design in seepage problems using dual integral formulation, *Finite Elements in Analysis and Design*, 17: 1-20.
- Deeks, A.J. and Chang, L. 2003. Potential flow around obstacles using the scaled boundary finite-element method, *International Journal for Numerical Methods in Fluid*, 28: 721-741.
- Fan, Y. and Tompkins, F.D. 1992. Generation of flow nets using F.E.M. nodal potentials and bilinear shape functions, *International Journal for numerical and analytical methods in Geomechanics*, 16: 427-435.
- Jie, Y. and Jie, G. and Mao, Z. and Li, G. 2004. Seepage analysis based on boundary-fitted coordinate transformation method, *Computers and geotechnics*, 31(4): 279-283.
- Lindemann, J. and Becker, W. 2002. Free-edge stresses around holes in laminates by the boundary finite-element method, *Journal of Geotechnical Engineering*, ASCE, 38: 407-416.
- Song, Ch. and Wolf, J.P. 1999. The scaled boundary finite-element method— alias consistent infinitesimal finite-element cell method-for diffusion, *International Journal for Numerical Methods in Engineering*, 45: 1403-1431.
- Wolf, J.P. and Song, Ch. 1996. *Finite-element modelling of unbounded media*, John Wiley and Sons, (Chichester).